Al-Azhar Bulletin of Science

Volume 34 | Issue 1 Article 6

2023

Section: Earth science

RESERVOIR CHARACTERIZATION OF HAMMAM FARAUN MEMBER IN NORTH EL MORGAN FIELD GULF OF SUEZ, EGYPT

Ahmed Walaan
Exploration Department, Gulf of Suez Petroleum Company, New Maadi, Cairo, Egypt, ahmed.walaan@hotmail.com

Alaa Mostafa
Geology Department, Faculty of Science, Al-Azhar University (Assiut Branch)

Mahmoud Hassaan
Exploration Department, British Petroleum Company (BP Egypt)

How to Cite This Article

Walaan, Ahmed; Mostafa, Alaa; and Hassaan, Mahmoud (2023) "RESERVOIR CHARACTERIZATION OF HAMMAM FARAUN MEMBER IN NORTH EL MORGAN FIELD GULF OF SUEZ, EGYPT," *Al-Azhar Bulletin of Science*: Vol. 34: Iss. 1, Article 6.
DOI: https://doi.org/10.58675/2636-3305.1634

ORIGINAL ARTICLE

Reservoir Characterization of Hammam Faraun Member in North El Morgan Field Gulf of Suez, Egypt

Ahmed Walaan [a,*], Alaa Mostaf [b], Mahmoud Hassaan [c]

[a] Department of Exploration, Gulf of Suez Petroleum Company, New Maadi, Cairo, Egypt
[b] Department of Geology, Faculty of Science, Al-Azhar University (Assiut Branch), Assiut, Egypt
[c] Department of Exploration, British Petroleum Company (BP Egypt), Egypt

Abstract

The main purpose of this work is to detect reservoir characterization of Hammam Faraun member of Belayim formation at North El Morgan oil filed based on integration of petrophysical and sedimentological studies. The work-flow in this study integrates multiple data evaluation techniques and multiple data scales by using a comprehensive interpretation of the available conventional, advanced digital well log data (large scale) and core analysis data (small scale). The petrophysical work shows the hydrocarbon saturation, shale volume and effective porosity are varied along reservoir. The NMR logs shows various clay bound volume, capillary bound water volume and free fluid content along the reservoir. The sedimentological work done includes core sample description, core log and ditch cutting description, that helped to understand facies distribution along reservoir zones, depositional cycles recorded in reservoir zones, relationship between different rock type and understanding the heterogeneity of the reservoir. Integrated petrophysical and sedimentological work lead to divide Hammam Faraun reservoir in to three zones (Hammam Faraun B1, B2 and B3 zones) which have different reservoir quality, facies type and lead to understand the behavior and production performance of each zone along area of study. By using petrophysical and sedimentological results we can outline possible opportunity areas as well as generate depletion development plan for the field to help in increasing field production through drilling new development wells and water injection wells.

Keywords: Core, El morgan oil field, NMR logs, Reservoir characterization

1. Introduction

El Morgan field is located in the Southern part of the Gulf of Suez; the field center is about 20 Km East of Ras Shukheir base, 13 Km North West of El-Tor town and 40 Km SE of Ras Gharib town (Fig. 1) and the field covers an area of about 46 Km^2 [1]. El Morgan field is one of the biggest oil field in Gulf of Suez and Egypt. Most of the oil reserves of El Morgan field are contained in the middle Miocene Kareem formation, minor production comes from the overlying sandstones of the upper Miocene Hammam Faraun member of Belayim formation (Fig. 2) and minor reserves are contained in the lower Miocene Rudeis formation LaChance and Winston, El Ayouty [2,3]. The well logging analysis used in the study represents the most important stage in the evaluation of petrophysical characteristics which involve shale content calculation, total porosity, effective porosity, water and hydrocarbon saturations as a conventional log analysis. The NMR logs identified fluid type and porosity types. The general purpose of well log analysis is to convert the raw log data into estimated quantities of oil, gas and water in the formation. The sedimentological work done include core description and facies analysis along reservoir.

Received 7 August 2022; revised 8 September 2023; accepted 10 September 2023.
Available online 3 October 2023

* Corresponding author at: Exploration Department, Gulf of Suez Petroleum Company, 2400 New Maadi, Cairo, Egypt.
E-mail address: ahmed.walaan@hotmail.com (A. Walaan).

https://doi.org/10.21608/2636-3305.1634

Fig. 1. Hydrocarbon occurrences in the Gulf of Suez, Egypt, showing the location of El Morgan Field (EGPC, 1996).

2. Geological setting of area of study

2.1. Stratigraphic framework

The Gulf of Suez stratigraphic framework can be divided into three major units depending on the rifting process that consider the main event affecting the topography and deposition of the Gulf of Suez strata (Fig. 2), a Prerift succession (Pre-Miocene or Paleozoic-Eocene), a Synrift succession (Oligocene-Miocene), Postrift succession (Post-Miocene or Pliocene-Holocene); Alsharhan [4]. The Belayim formation unconformably overlain the Kareem formation. Belayim formation is divided in to four members in the area of

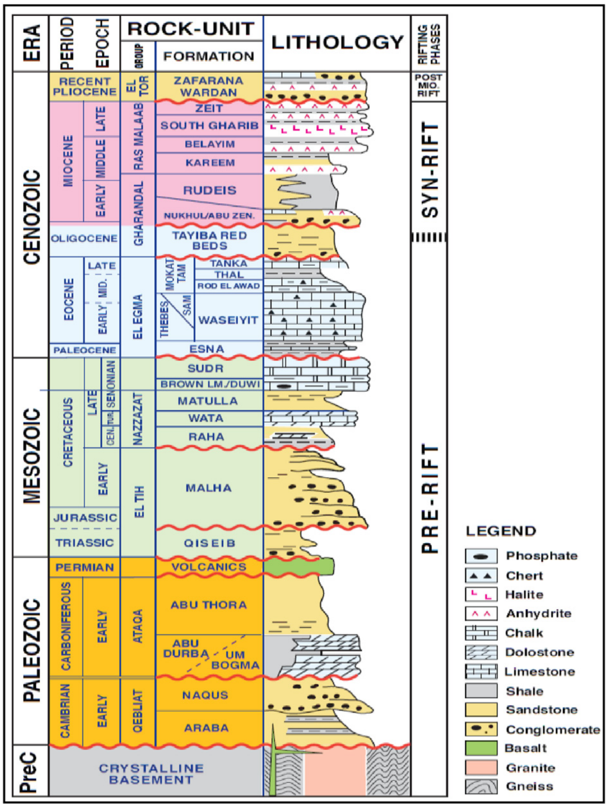

Fig. 2. General stratigraphy of the Eastern Gulf of Suez (Darwish, 1993).

study. The Hammam Faraun member is the uppermost which is the most productive unit and contains the majority of the reservoir in the Belayim formation. Underlying by Feiran member, mainly evaporites which underlying by Sidri member then at bottom Baba member which overlain Kareem formation. Hammam Faraun Member is usually referred to as 'Belayim classics' generally composed of sandstone with interbedded dolomitic silts and shale. In the Morgan area three coursing upward sequences have been identified which have been subdivided in to 10 unites. These deposits have been interpreted as channel lobs and levies from a prograding fan delta complex Paleontological data suggest a mid-shelf marine depositional environment in water depths ranging from 60 to 100 M. However, palynological data suggest a deeper depositional environment of inner to outer neritic in 100–200 M of water. Thickened classics section trend NW–SE along the West flanks of both north Morgan and Badri structures and thin over the structure crests [1].

2.2. Structural framework

The Red sea - Gulf of Suez rift system is a type - example of an intercontinental rift Landon [5] that was developed by the separation of the African and Arabian plates in Late Oligocene - Early Miocene time. The Gulf of Suez rift has been traditionally referred to as the clysmic rift Robson [6]. El Morgan field is located in the Morgan hinge zone Garbee and colleagues [7]. El Morgan field is an elongated North West trending anticline, the long axis of structure is some 13.7 Km long and short axis at widest part is some 5 Km long. The field bounded from Eastern border by Badri field and from Western border by Edfu and Saqqara fields. El Morgan and Badri fields complex are situated within one of the major transfer zones of Gulf of Suez. This conjugate convergent transfer zone links the Southern Gulf of Suez region (Fig. 3), where fault blocks are predominantly tilted to the WSW, to the central Gulf of Suez where fault blocks are tilted to the ESE [1]. El Morgan field comprises of two NW-trending tilted fault-blocks North and South El Morgan, probably separated at the main reservoir Kareem level by a Miocene erosional channel (Saddle) filled with Belayim evaporites Hady and colleagues [8].

3. Material and methods

Using three wells; named M118, M246 and M147 (Fig. 4 & Table 1), the available data in this study comprises.

(1) Conventional logs- The North El Morgan field wells have a full set of conventional logs that include Gamma ray, Resistivity, Density, Neutron, Sonic, and Photo electric factor (PEF).
(2) Advanced logs- Two wells (have Nuclear Magnetic Resonance logs (NMR).
(3) Core Data- Core reports for one well have been used to calibrate the petrophysical analysis.

3.1. Petrophysical methods

The objective of petrophysical analyses is to calculate shale volume, total porosity, effective porosity, water saturation, permeability, net pay thickness and net to gross ratio of the reservoir sections (Fig. 5) petrophysical analysis work flow. NMR logs to identify fluid type and kind of fluid contain in pore space.

3.1.1. Shale volume (V_{sh}) calculation

It is defined as the percentage of shale (clay) content that present in the reservoir rocks and considered as the most important parameter that effects on the porosity, permeability and saturation calculations. The preferred method for shale volume

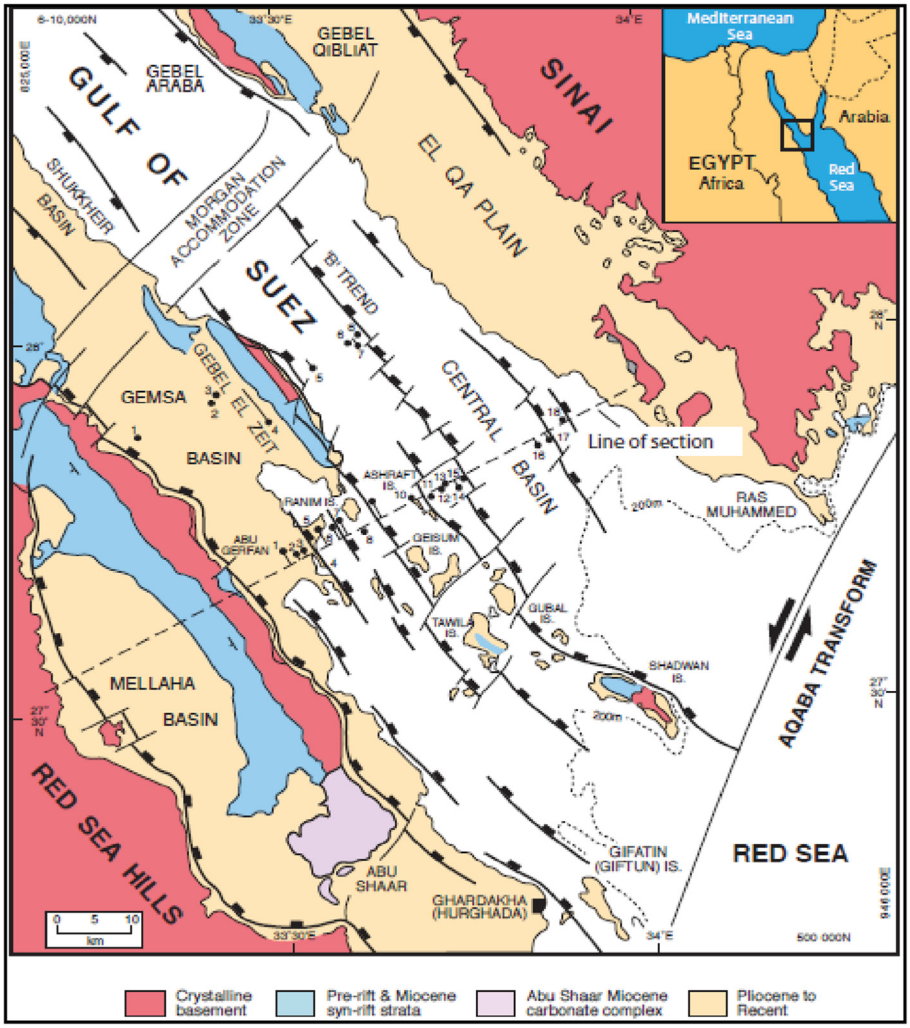

Fig. 3. Summary map of the Southern Gulf of Suez show El Morgan accommodation zone (after Bosworth, 1994).

calculation is the Neutron-Density method because the sandstone of Hammam Faraun reservoir is feldspathic sand and rich with feldspar content which effect on (GR) reading, so the best methods for (V_{sh}) calculation is the Neutron - Density method (Eq. (1)).

$$VSHND = (\phi N - \phi D) / (\phi NSH - \phi DSH) \qquad \text{(Eq.1)}$$

Where:-

ΦN = Neutron porosity in the sand.
ΦD = Density porosity in the sand.
ΦNSH = Neutron porosity in adjacent shale.
ΦDSH = Density porosity in adjacent shale.

3.1.2. Total porosity (Øt) determination

Porosity is defined as the ratio of the volume of void or pore space (Vp) to the total of the bulk volume (Vt) of the rock, there are three log-derived porosity measuring tools in common use that are density, neutron and sonic log, or combination of density and neutron Poupan and Gaymard [9]. which used in this study applying the following equation (Eq. 2).

$$\Phi ND = (\Phi N + \Phi D) / 2 \qquad \text{(Eq.2)}$$

Where: -

ΦND = Porosity from density/neutron logs.
ΦD = Porosity from density log.
ΦN= Porosity from neutron log.

3.1.3. Effective porosity (Øeff) determination

It is the volume of interconnected pore spaces per bulk volume of the rock. The shale volume and corrected total porosity have an effect on effective porosity value, the effective porosity calculated for shaly and clean zones using density and neutron logs Schlumberger [10] applying the following formula (Eq. 3).

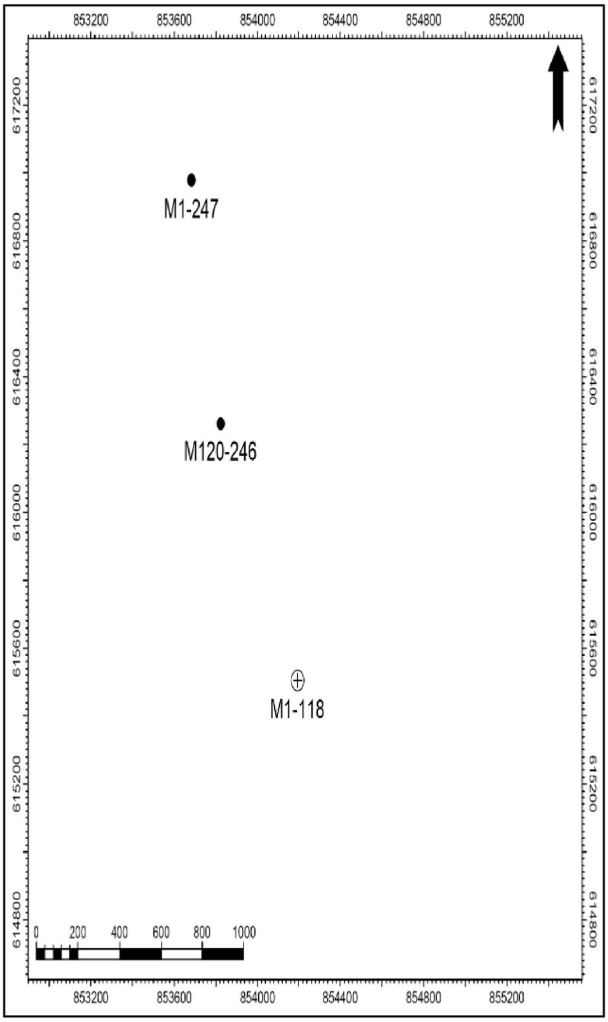

Fig. 4. Location map for selected wells in the area of study.

$$\Phi eff = \Phi t - (Vsh \times \Phi sh) \qquad \text{(Eq.3)}$$

Where:-

Φ_{eff} = Effective porosity.
Φ_t = Total porosity.
Φ_{sh} = Neutron porosity in 100% shale.
V_{sh} = shale volume.

3.1.4. Permeability (k) determination

The permeability was determined using three different sources (Core, NMR and conventional

Table 1. Wells Coordinates in the area of study.

Well Name	Coordinates	
	Start point	End point
M247	X: 854,022.99 m E Y: 615,963.00 m N	X: 853,681.17 m E Y: 616,978.74 m N
M246	X: 853,793.99 m E Y: 615,410.00 m N	X: 853,822.91 m E Y: 616,260.37 m N
M118	X: 854,023.00 m E Y: 615,963.00 m N	X: 854,183.100 m E Y: 615,517.98 m N

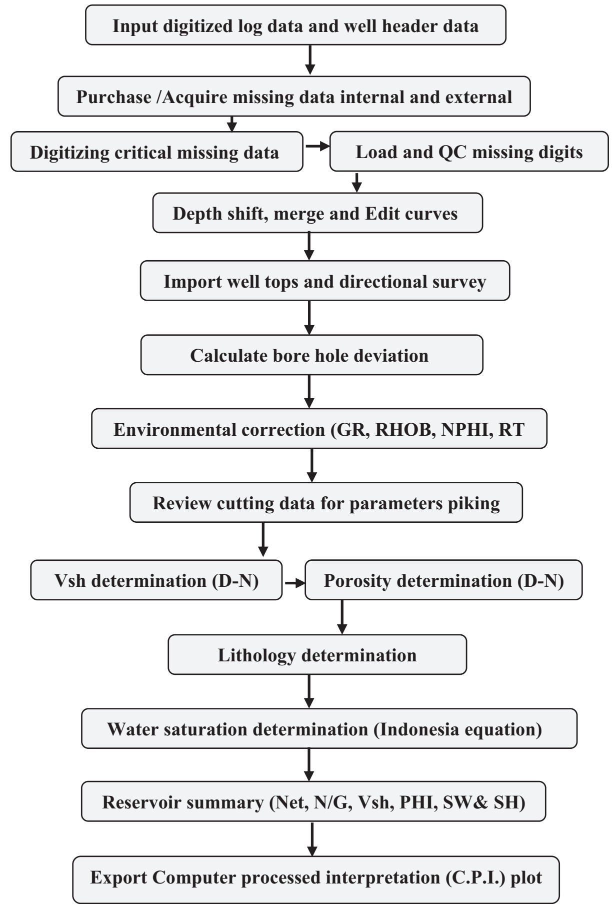

Fig. 5. Simplified work flow chart of the applied petrophysical evaluation.

logs). Conventional open-hole log interpretation can provide total and effective porosities, but cannot state the free fluid porosity, and permeability. As a new technology NMR wireline tool can provide the important reservoir parameters like permeability and pore radius Dhar [11]. NMR is a technology that is able to yield a huge amount of information about the reservoir characteristics Straley and colleagues [12]. NMR measures the relaxation time (T2) of hydrogen protons in a porous medium after applying a magnetic field sequence. The relaxation time is proportional to a pore size distribution where large pores show long T2 and small pores show short T2. Thus, a T2 cutoff value can be applied to differentiate between bound (small pores) and moveable (larger pores) fluids Coates and colleagues [13]. It was reported that the bound water cutoff value for sandstones is about 33 MS Timur [14]. In Hammam Faraun sandstone reservoir the standard sandstone T2 cutoff of 33 MS (red line) was used (Figs. 6 and 7). The NMR estimates permeability based on the model which shows that permeability increases with increase of both porosity and pore size Timur [15]. The permeability was also determined from conventional logs using the elemental analysis model.

3.1.5. Formation water resistivity (R_w) determination

It is the resistivity of water found in pores spaces of porous formation. Salinity and Temperature consider as one of the most important factors controlling and affecting on formation water resistivity (Rw) determination. The higher salinity gives low resistivity reading and vice versa and higher temperature gives low resistivity and vice versa. The important two methods are used to determine the (Rw), the first method is water sample measurement and the second method is the graphical technique, resistivity-porosity computations cross plot Pickett [16].

Formation water Resistivity (R_w) determination by using direct measurement of water samples: Its direct measurement method that depends on measuring the salinity of formation water sample (from drill stem test, core analysis data, wire line formation tester or produced water from producer wells without (injection effect) at certain temperature, then an equivalent NaCl concentration is obtained,

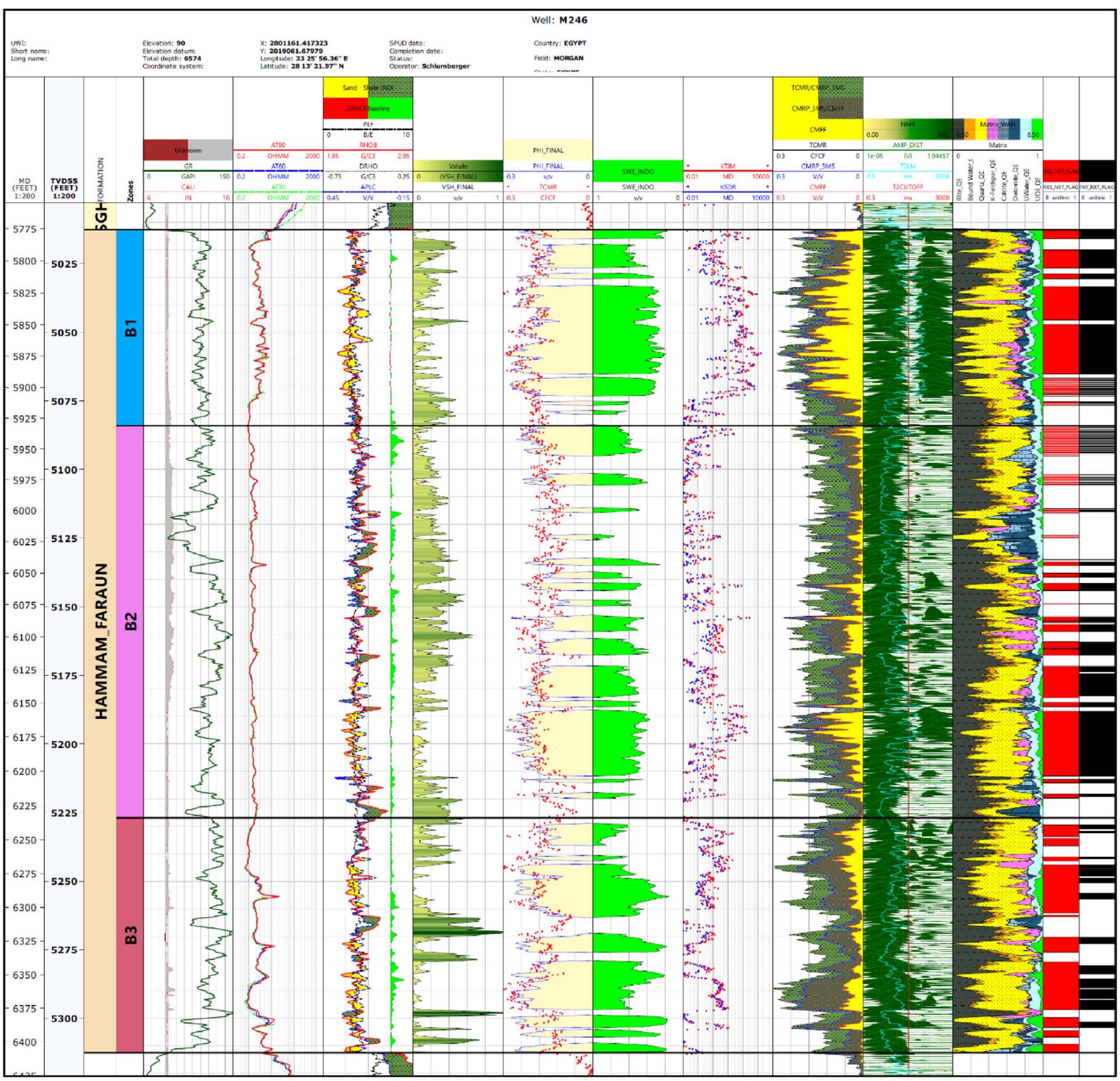

Fig. 6. Computer processed interpretation (C.P.I.) plot for Hammam Faraun reservoir in M246 well.

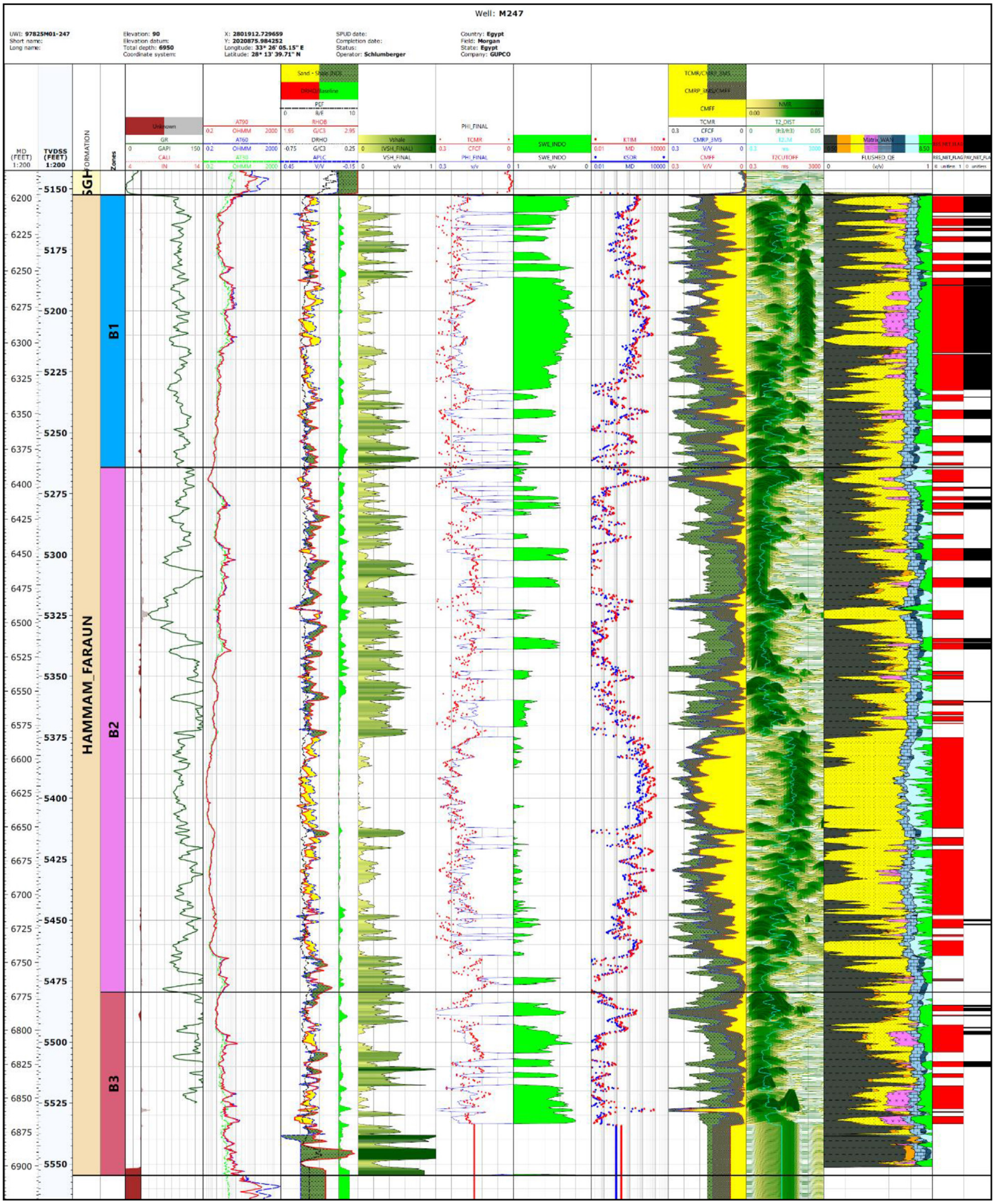

Fig. 7. Computer processed interpretation (C.P.I.) plot for Hammam Faraun reservoir in M247 well.

that is used in calculating (Rw) by Schlumberger resistivity of NaCl water solutions chart. The average (R_w) used in this study is 0.024ohmm.

3.1.6. Water saturation (S_w) determination

The Water saturation is the fraction of the pore volume of the reservoir that is filled with water, its symbol is (S_w), various subscripts are used to denote saturation of a particular fluid, (S_w) is water saturation, (S_h) is hydrocarbon saturation, the summation of all saturations in a given formation of rock must totally be 100% Schlumberger [17]. Indonesia method Poupon and Leveaux [18] is used in this study because Hammam Faraun thin laminated reservoir, highly shale content reservoir as the following equation (Eq. 4).

$$S_w = \left\{ \left[\left(\frac{V_{sh}^{2-V_{sh}}}{R_{sh}} \right)^{\frac{1}{2}} + \left(\frac{\Phi_e^m}{R_w} \right)^{\frac{1}{2}} \right]^2 R_t \right\}^{\frac{-1}{n}} \tag{4}$$

Where:

Sw = Water saturation of the un-invaded zone.

Rw = Formation water resistivity at formation temperature.

Rt = True formation resistivity (deep resistivity).

Φ = Total Porosity.

A = Tortuosity factor.

M = Cementation factor.

N= Saturation exponent.

Vsh = Volume of shale.

Rsh = Resistivity of shale.

Φeff = Effective porosity of the formation.

* Reservoir cut off used in this study, $\Phi_{eff} = 10\%$ Minimum, $S_w = 70\%$ Maximum, $V_{sh} = 35\%$ Maximum based on field experience, A = 1, M = 1.9 & N = 2; based on special core analysis data.

3.1.7. Petrophysical results and discussion

The integrated conventional and advanced logging analysis showed that Hammam Faraun reservoir is a heterogeneous reservoir where sandstone quality showed lateral and vertical quality change. Hammam Faraun reservoir an excellent example of thin laminated sandstone sequence; where, this sequence within Belayim formation is composed of calcite and dolomite rich mudstone intercalated with fine to medium grained sandstone.

The Hammam Faraun reservoir in M246 well shows good reservoir quality for B1 zone, which have 70% net to gross, 11% average shale content, 21% average porosity and 65% average hydrocarbon saturation (Table 2a & Fig. 6). NMR logs showed that the calculated water volume from conventional logs has a good match with the estimated irreducible water volume from NMR. In addition to porosity with a good match with calculated from conventional logs, there are increasing in free fluid content in pores matched with permeability than capillary bound fluid volume and clay bound fluid volume, which led to a high possibility of producing oil free water. The B2 zone showed 51% net to gross, with 11% average shale content, 20% average porosity and 45% average hydrocarbon saturation. The B2 zone shows poor reservoir quality at top and middle part where increasing in shale content and low permeability values. NMR logs showed increasing in clay bound and capillary bound water than free fluid content and low permeability, which minimize production rate. The B3 zone shows 70% net to gross, 7% average shale content, 21% average porosity and 53% average hydrocarbon saturation. NMR logs shows increasing in capillary bound water and clay bound fluid than low free fluid content and low permeability values along zone, that interpret saturation comes from capillary fluid than free fluid, which minimize production rate for current zone.

The M247 well shows good reservoir quality for B1 zone, which have 69% net to gross, 10% average shale content, 20% average porosity and 56% hydrocarbon saturation. Computer processed interpretation (CPI) plot (Table 2b & Fig. 7) shows high reservoir quality at middle part where low shale content and good porosity. NMR logs showed increasing in free fluid content in pores matched with permeability than capillary bound fluid volume and clay bound fluid volume, which led to a high possibility of producing oil free water. The B2

Table 2b. Summary of petrophysical parameters for Hammam Faraun reservoir in M247 well.

	B1	MD	6198	6388	190	131	69	10	20	44	56
		TVD	5241	5352	112	77					
M247	B2	MD	6388	6772	384	211	55	9	20	86	14
		TVD	5352	5568	215	120					
	B3	MD	6772	6907	135	56	41	11	19	47	53
		TVD	5568	5643	75	31					

Table 2a. Summary of petrophysical parameters for Hammam Faraun reservoir in M246 well.

Well	Zone	Depth	Top (ft)	Bottom (ft)	Gross (ft)	Net (ft)	Net/Gross (%)	Vsh (%)	Øeff (%)	Sw (%)	Sh (%)
M246	B1	MD	5776	5931	155	108	70	11	21	35	65
		TVD	5103	5174	71	50					
	B2	MD	5931	6234	303	153	51	11	20	55	45
		TVD	5174	5317	143	73					
	B3	MD	6234	6408	174	121	70	7	21	47	53
		TVD	5317	5403	86	60					

Table 2c. Summary of petrophysical parameters for Hammam Faraun reservoir in M118 well.

	B1	MD	5256	5331	75	25	33	14	19	39	61
		TVD	5029	5102	72	24					
M118	B2	MD	5331	5474	143	35	24	14	19	49	51
		TVD	5102	5239	138	34					
	B3	MD	5474	5540	66	19	29	13	15	75	25
		TVD	5239	5302	63	18					

zone shows 55% net to gross, 9% average shale content, 20% average porosity and 14% average hydrocarbon saturation, Resistivity curve showed oil water contact (OWC) @ −5335 ft TVDss where most of B2 zone water bearing reservoir. The B3 zone showed 41% net to gross, 11% average shale content, 19% average porosity and 53% average hydrocarbon saturation. Computer processed

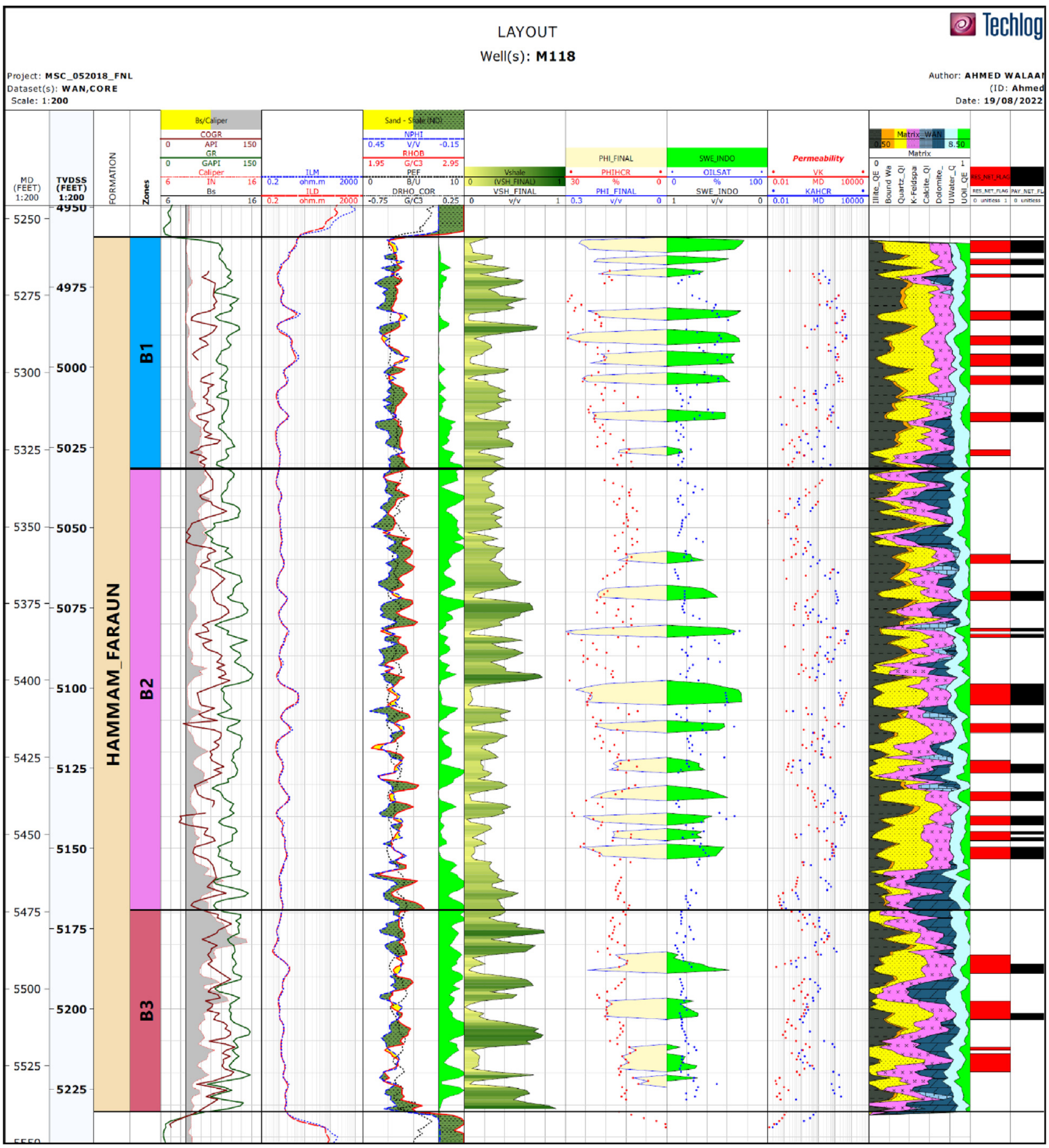

Fig. 8. Computer processed interpretation (C.P.I.) plot for Hammam Faraun reservoir in M1-118 well.

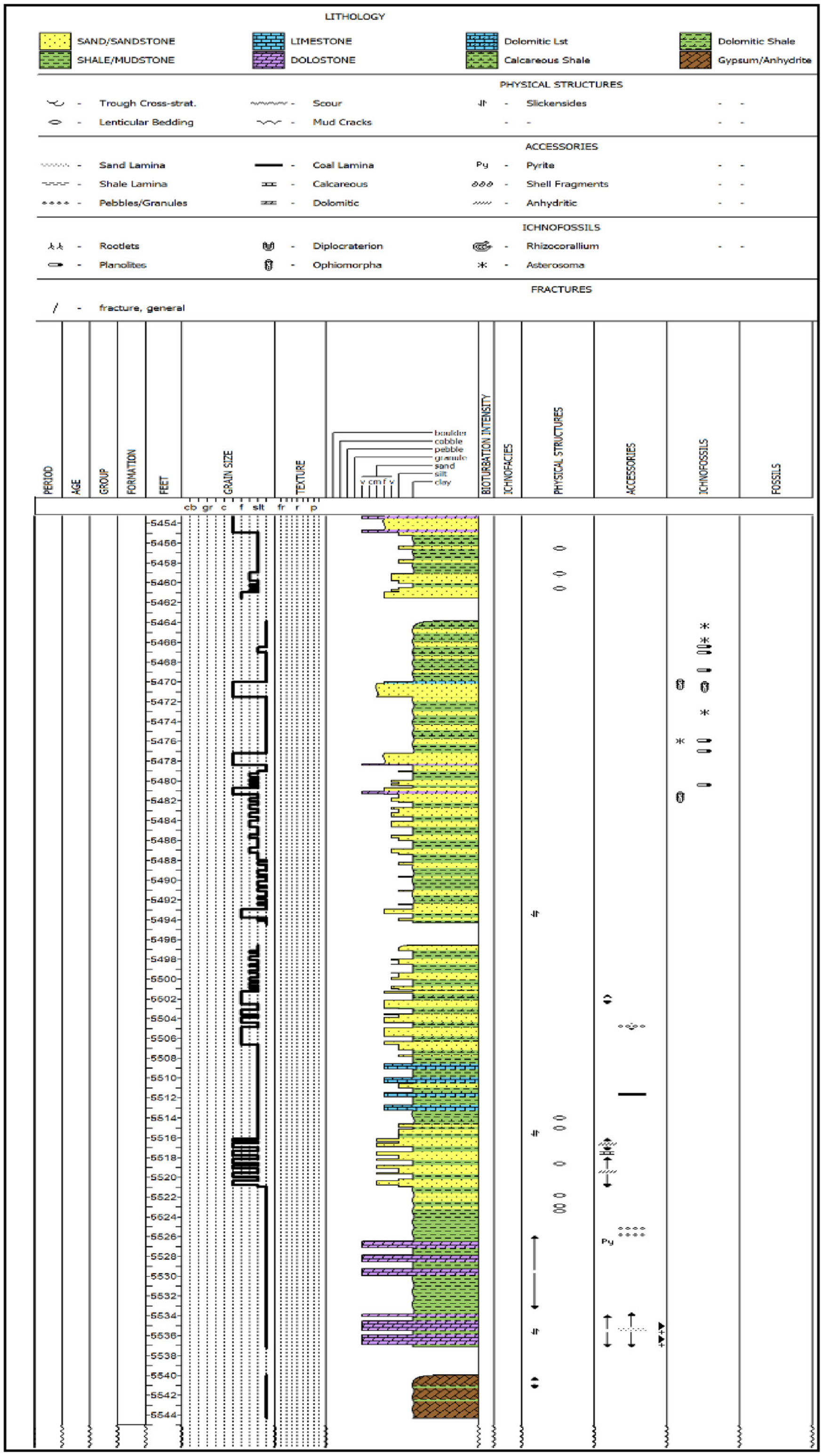

Fig. 9. Core description and facies analysis log for units (A & B).

interpretation (CPI) plot (Fig. 7) shows low reservoir quality although conventional logs shows good hydrocarbon saturation, good porosity and low shale contents, where NMR logs shows increasing in clay bound volume, capillary bound water volume and low free fluid content which minimize production rate and performance of B3 zone.

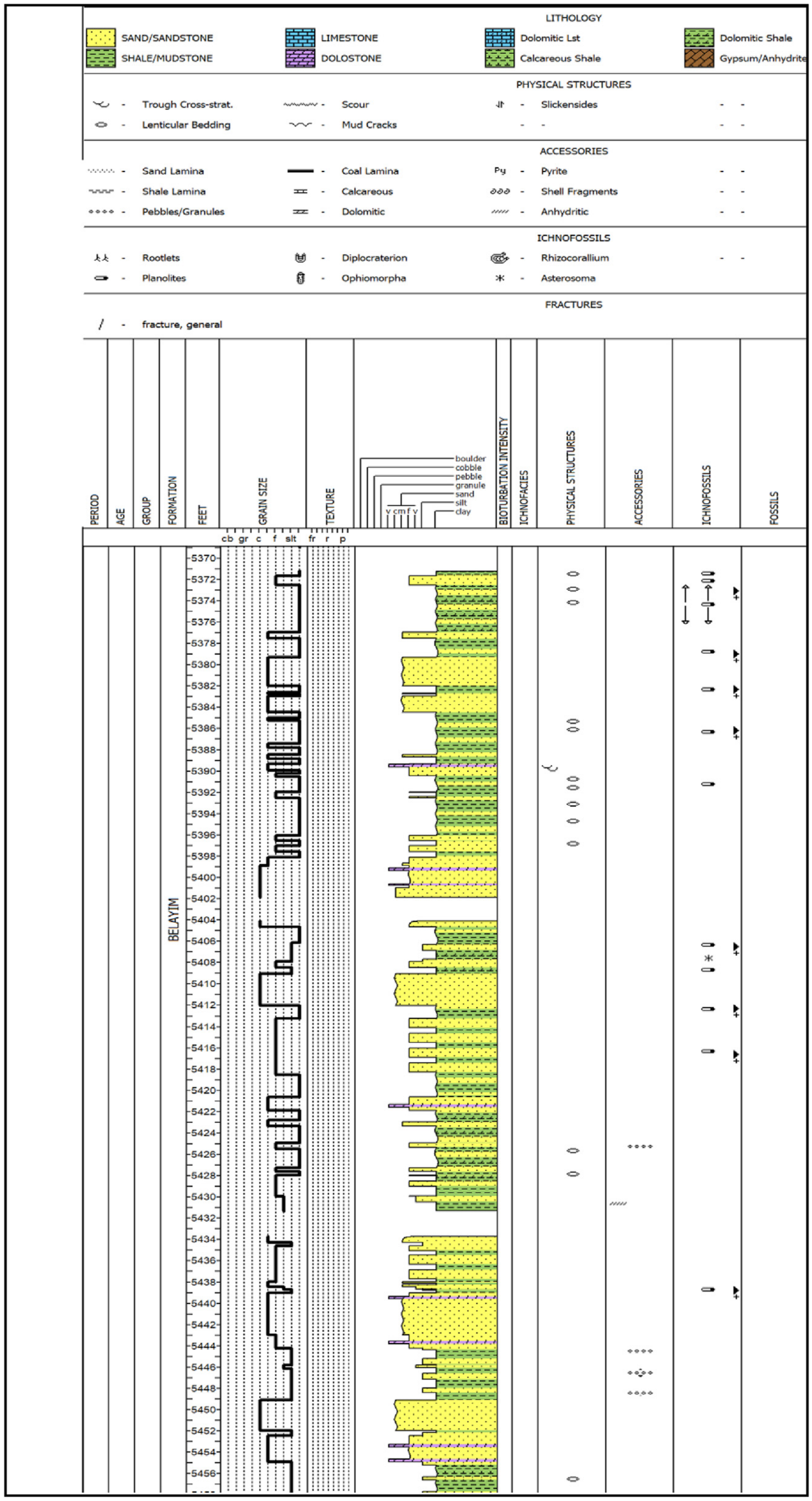

Fig. 10. Core description and facies analysis log of unit (C).

The M118 well B1 zone shows 33% net to gross, with 14% average shale content, 19% average porosity and 61% hydrocarbon saturation. Integrated petrophysical analysis with core showed good match in porosity, hydrocarbon saturation and low net to gross reservoir an excellent example of

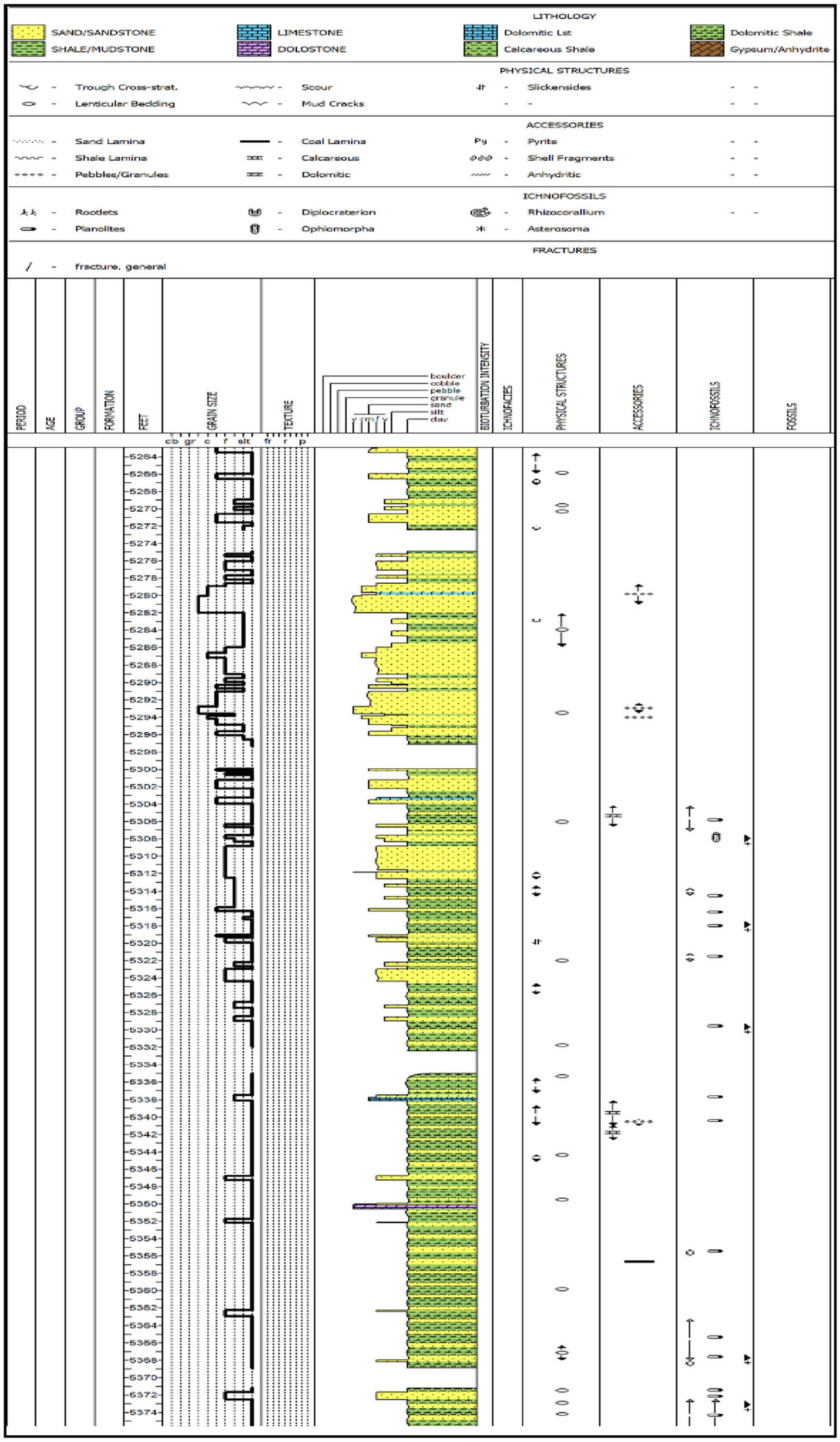

Fig. 11. Core description and facies analysis log of unit (D & E).

thin laminated sandstone sequence (Table 2c & Fig. 8). The B2 zone shows 24% net to gross, with 14% average shale content, 19% average porosity and 51% average hydrocarbon saturation. Computer processed interpretation (CPI) plot showed low reservoir quality, highly shale content and low porosity at top part and intermediate reservoir quality where enhance in porosity and sandstone percentage at middle to basal part. There is a good matching in core data and petrophysical data. The B3 zone shows 29% net to gross reservoir, with 13% average shale content, 15% average porosity and 25% average hydrocarbon saturation. Computer processed interpretation (CPI) showed low reservoir quality where highly shale content, fair porosity, low-scattered permeability, low hydrocarbon saturation matched with core data.

The Hammam Faraun reservoir generally good quality reservoir for B1 zone which share main production of the reservoir. The B2 zone shows intermediate to good reservoir quality with good net to gross reservoir thickness. The B3 zone shows low reservoir quality and hydrocarbon saturation in conventional log analysis recognized from NMR as capillary bound fluid, nonproduced fluid.

3.2. Sedimentological analysis

The sedimentological studies show that the Hammam Faraun reservoir consists generally of sandstone with interbedded dolomitic silts and shale. The Hammam Faraun reservoir in North Morgan filed thickness ranged from 300 to 600 ft.

3.2.1. Core description

M118 well is the only one that had cored within the Hammam Faraun member section in the study area. Five contentious conventional cores had collected during the drilling of this well, the cored interval in Hammam Faraun member is a thick 282 ft. The lithology of cored interval unit (A) bottoms part it is consisting of anhydrite and mud clast breccia within a mudstone matrix and slickensides present. The

Table 3a. Photographs and a summary description of Hammam Faraun reservoir sandstone facies.

Color	Facies Name	Photo	Description
	Facies (A)		Facies (A): Coarse to very coarse sandstone, occasionally grading to conglomerates, loose, poorly sorted, immature, thick bedded, located in upper fan as depositional environment
	Facies (B)		Facies (B): Medium to coarse sandstone, sub mature, with calcareous cement, hard, dispersed clay moderately to pore sorted, coarsening upward, prograding mid fan as depositional environment.

unit from 5540 ft to 5533 ft consists of anhydrite with deformed laminations of mud above 5542 ft (Fig. 9). The unit (A) is the basal part of Hammam Faraun reservoir, conformably overlying Feiran member. The lithology of cored interval unit (B) The unit consists of carbonate rich and noncarbonate mudstones interlayered with siltstones and very fine to medium grained sandstones. Sandstones, which make up 14% of the unit are within layers ranging in thickness from less than 0.5 ft. to greater than 1.5 ft. thick beds (Fig. 9). The lithology of cored interval unit (C) The unit consists primarily of fine to coarse grained sandstone interlayered with carbonate and noncarbonate rich mudstone. Mudstone, which make up to 52% of interval, contains physical sedimentary structures such as laminations, ripple beds, and lenticular ripple beds (Fig. 10). Traces fossils are present at irregular intervals and consist of Asterosoma and Planolites. Sandstone beds, ranged in thickness from less than 0.5 ft to over 3.5 ft. Structures present within the sandstones are large scale cross-bedding and mud clasts and some of the beds are graded. - The lithology of cored interval unit (D) The unit consists primarily of calcite and dolomite rich mudstone with only few beds of very fine to fine grained sandstone (5%). Sedimentary structures present are laminations, ripple bedding and lenticular ripple beds (Fig. 11). Traces fossils are present in some intervals and consist of Planolites and Asterosoma. Based on petrographic analysis,

Table 3b. Photographs and a summary description of Hammam Faraun reservoir sandstone facies.

Facies (C)		Facies (C): Medium to fine grains sandstone, mature, with calcareous cement, dispersed and laminated mudstone, anhydrite clast, moderately to well sorted, massive bedded, fining upward mid fan delta as depositional environment.
Facies (D)		Facies (D): Fine to very fine sandstone, mature, silty sandstone, laminated with high silt intercalations, common dispersed and laminated mudstone, anhydrite clast, argillaceous and dolomitic cement, well sorted.

mudstones contain abundant dolomite up to 41%, calcite up to 14%. The lithology of cored interval unit (E) The unit consists of calcite rich mudstone interlayered with fine to very coarse-grained sandstone (Fig. 11). Sandstone which make up 30% of the interval, contain some laminations, ripple beds and trace fossil such as Ophiomorpha, Asterosoma and Planolites. Trace fossils present within the mudstone primarily Planolites and no burrow traces observed above 5300 ft MD.

3.2.2. Facies analysis

The Hammam Faraun reservoir shows four sandstone dominated lithofacies that identified based on petrographic analysis from core samples (Tables 3a and b).

Sandstone facies (A); Descripted as coarse to medium grains occasionally very coarse grains, loose texture, friable, very low to negligible cementation, moderately sorting and immature sandstone. Good reservoir quality and distributed along Hammam Faraun B2 and B1 zones (Table 3a).

Sandstone facies (B); Descripted as coarse to medium grains sandstone, with calcareous cement and occasionally loose texture, dispersed clay, moderately to poorly sorting, immature, highly feldspars content, feldspars clay alteration and leaching, preserved pores and quartz overgrowth. Good to medium reservoir quality and distributed along Hammam Faraun B2 and B1 (Table 3a).

Sandstone facies (C); Descripted as medium to fine grains sandstone, calcareous cementation, dispersed clay, poorly sorting, immature, highly feldspars content, preserved pores. Medium to poor reservoir quality and common in Hammam Faraun B3 and B2 zones (Table 3b).

Sandstone facies (D); Descripted as fine to very fine grains sandstone, calcareous and argillaceous cement, poorly sorting, immature, highly feldspars content, dolomitic rich content and rock fragments. Poor reservoir quality and common in Hammam Faraun B3 zone (Table 3b).

4. Conclusions

Integrated petrophysical (conventional & advanced) and sedimentological study of Hammam Faraun reservoir clearly identified that the reservoir is heterogeneous reservoir, based on the micro and macroscopic heterogeneity scales and thin laminated sandstone characterized with low net to gross reservoir. The reservoir divided in to three zones (B1, B2 and B3) based on integration study for both petrophysical and sedimentological, B1 zone top of reservoir which showed good reservoir quality and share main production of reservoir. B2 zone which separated vertically from B1 with thick shale intercalation as vertical barrier, B2 zone showed intermediate to low reservoir quality at top part characterized with highly shale content and very thin sand layers, with going down reservoir showed enhance in quality to be good reservoir quality at middle to bottom part, B2 share same production performance as B1 zone of reservoir. The B3 zone which is the base part of reservoir zone didn't share production rate across the field and clearly identified in the current study that hydrocarbon saturation comes from conventional logs as tar, heavy oil non producible, NMR logs showed increasing in capillary bound water volume, clay bound volume and low free fluid content across B3 zone in recorded wells which minimize/limited production rate and performance of B3 zone.

Conflicts of interest

The authors approve that no conflicts exist.

Acknowledgements

The authors very much thank EGPC (Egyptian General Petroleum Corporation) and GUPCO (Gulf of Suez Petroleum Company) for giving the data needed for this work and permissions for publication. Many thanks to GUPCO Petrophysicist and Petrologist team for giving access to Labs with the needed software and facilities.

References

[1] Egpc. Gulf of Suez oil fields (a comprehensive overview). Cairo: Egyptian general petroleum corporation; 1996. p. 35–41.
[2] LaChance DP, Winston RT. Recognition of waterflood sweep and formation lithology in a giant Egyptian oil field by applied petrophysics. SPE Form Evaluation 1987 Jun 1;2(02): 150–4. Las Vegas, USA.
[3] El Ayouty MK. Petroleum geology. In: Said R, editor. The geology of Egypt. Rotterdam: A.A. Balkema; 1990. p. 567–98.
[4] Alsharhan AS. Petroleum geology and potential hydrocarbon plays in the Gulf of Suez rift basin, Egypt. AAPG (Am Assoc Pet Geol) Bull 2003;87:143–80.
[5] Landon S. Interior rift basins. AAPG 1994;54:1–4.
[6] Robson DA. The structure of the Gulf of Suez (Clysmic) rift, with special reference to the eastern side. J Geol Soc 1971; 127:247–76.
[7] Garbee MH, Coffield DQ, Perry SK, Schamel S, Smale JL. Structure of morgan hinge zone, Gulf of Suez, Egypt. AAPG (Am Assoc Pet Geol) Bull 1986;70:593.
[8] Hady IA, Rady M, Woodward DE. An application of engineering and geological technologies to improve production performance in the Kareem reservoir of North El Morgan Field. In: Bahrain: proceedings SPE 10th middle east oil show; 1997. p. 255–63. SPE 37785.
[9] Poupan A, Gaymard R. The evaluation of clay content from logs. SPWLA 11th annual logging symposium. 1970.
[10] Principles S. The essential of log interpretation practice. Paris France; 1972.

[11] Dhar SK. Reservoir characterization of Gandhar pay sands by integrating NMR log data with conventional open hole logs e a case study. In: International conference & exposition on petroleum geophysics, Kolkata, 6; 2006. p. 7.
[12] Morriss C, Rossini D, Straley C, Tutunjian P, Vinegar H. Core analysis by low-field NMR. Log Analyst 1997 Mar 1; 38(02). Stavanger, Norway.
[13] Coates G, Xiao L, Prammer M. NMR Logging principles and applications. USA: Haliburton energy services; 1999.
[14] Timur A. Nuclear magnetic resonance study of carbonate rocks. Log Anal 1991;13:518−35.
[15] Timur A. Effective porosity and permeability of sandstones investigated through nuclear magnetic principles. Log Anal 1969;10:1.
[16] Pickett GI. A review of current techniques for determination of water saturation from logs. J Petrol Technol 1966;18: 1425−33.
[17] Schlumberger. Log interpretation, principles/application. 1989.
[18] Poupon A, Leveaux J. Evaluation of water saturation in shaly formations. In: Proceedings of the SPWLA 12th annual logging symposium; 1971.